ATF Beamline 1
Analysis Spectrometer

R. C. Fernow, H. G. Kirk and S. Ulc

Physics Department

Brookhaven National Laboratory
Associated Universities, Inc.
Upton, Long Island, New York 11973

MASTER

ATF Beamline 1
Analysis Spectrometer

R.C. Fernow, H.G. Kirk & S. Ulc

January 1993

We describe the design parameters and expected
performance of the analysis spectrometer for beamline 1
at the BNL Accelerator Test Facility. The spectrometer
should be well suited for measuring the change in energy
caused by the first generation laser acceleration
experiments.

1 Overview

The ATF beamline 1 analysis spectrometer is intended primarily for
measuring the energy gain in the advanced acceleration experiments.
The Inverse-Cerenkov Acceleration[1] and Grating Acceleration[2]
experiments, currently approved for running on this beamline, will
use the spectrometer for this purpose. In addition other
experiments, like the Nonlinear-Compton scattering experiment[3],
can use the spectrometer as a monitor of the electron beam-laser
interaction.

The basic layout of the spectrometer is shown in Fig. 1. The beam
leaving an interaction region encounters a vertically bending
dipole, which is used to disperse the beam transversely as a
function of momentum. Three quadrupoles, located in the space
between the dipole exit face and the detector, are used to control
the focal spot at the detector[4]. The detector is a modified
Princeton profile monitor and is described in section 3. Following
the detector is a Faraday cup for measuring the charge in each beam
bunch.

Fig. 1

The initial set of acceleration experiments will not be able to control the phase of the interaction between the laser and the electrons. As a consequence the result of the interaction will be that some electrons will be accelerated, some decelerated, and others will be deflected. This means that the center of the spot produced on the detector will not move relative to a shot with the laser turned off, provided that the dipole is set to accept the mean incident beam momentum and that the experimental conditions are stable. Thus for these early measurements, where the total momentum change is no more than ≈1 MeV/c, one is mainly interested in the width of the signal on the detector. The absolute location of the spot on the detector is determined by the mean beam momentum and is only of secondary importance for this measurement. All the essential information about the interaction comes from the size and shape of the spot itself, wherever the spot may lie on the detector plane. This is important because it means we can tolerate a certain amount of jitter from vibrations, magnet current variations, beam position drifts, etc. and not affect the spectrometer measurement.

When the experiments produce momentum gains larger than ≈1 MeV/c, it will no longer be possible to see the entire distribution on the profile monitor at one time. In this case it will be necessary to use the spectrometer for an absolute measurement of momentum. The limits of the energy change distribution must be determined by changing the dipole field gradually until no further particles are seen on the profile monitor.

The strategy for the quadrupole settings is to have a point to point focus in the bending plane of the dipole. If we assume that the interaction region is small, all particles leaving with a given momentum are focused to a point on the detector, regardless of their initial divergence in that plane. However, particles with different momenta are focussed to different locations at the detector. Thus the location of the detector spot gives us information about the momentum change of the particles, but information about any deflections caused by the interaction in the bend plane will be lost. The quad tune in the non-bend plane should be roughly point to parallel, the main criterion being that the beam fall on the detector. The location of a trajectory at the detector in the non-bend direction should be proportional to the divergence in that direction caused by the interaction. Higher order effects in the magnetic optics will modify these statements to some extent.

Some dimensional properties of the spectrometer are indicated in Table 1.

Table 1 Spectrometer dimensions			
element	length	Σlength	R_p
	cm	cm	mm
L1	8.7	8.7	
GD2	28.2	36.9	
L2	63.9	100.8	
GQ14	10.2	111.0	15.2
L3	15.0	126.0	
GQ15	20.4	146.4	15.2
L4	15.0	161.4	
GQ16	10.2	171.6	15.2
L5	20.0	191.6	
L6	24.2	215.8	

L1 is the distance from the beam pipe flange to the dipole magnetic entrance edge. L5 is the distance from the last quad exit magnetic edge to the profile monitor screen. L6 is the distance from the screen to the entrance of the Faraday cup collection plate.

The beam pipe inner diameter between components in the spectrometer is 25.3 mm. The smallest beam aperture is the entrance and exit beam pipes to the dipole vacuum chamber, where the inner diameter is 19.05 mm.

2 Magnetic measurements

A circular coil dipole was used in the analysis spectrometer. The steel pole piece shown in Fig. 2 was designed for normal entrance and exit with a nominal bend angle of 25°. The edge of the pole was tapered such that the magnetic effective edge of the magnet would correspond with the physical edge. Although the measured angle between the entrance and exit pole edges was 24°48', the entrance and exit beam pipes were surveyed at 25°. The gap between the dipole pole pieces is 3.099 cm. The distance from the edge of the dipole pole piece to the theoretical bend point is 14.321 cm.
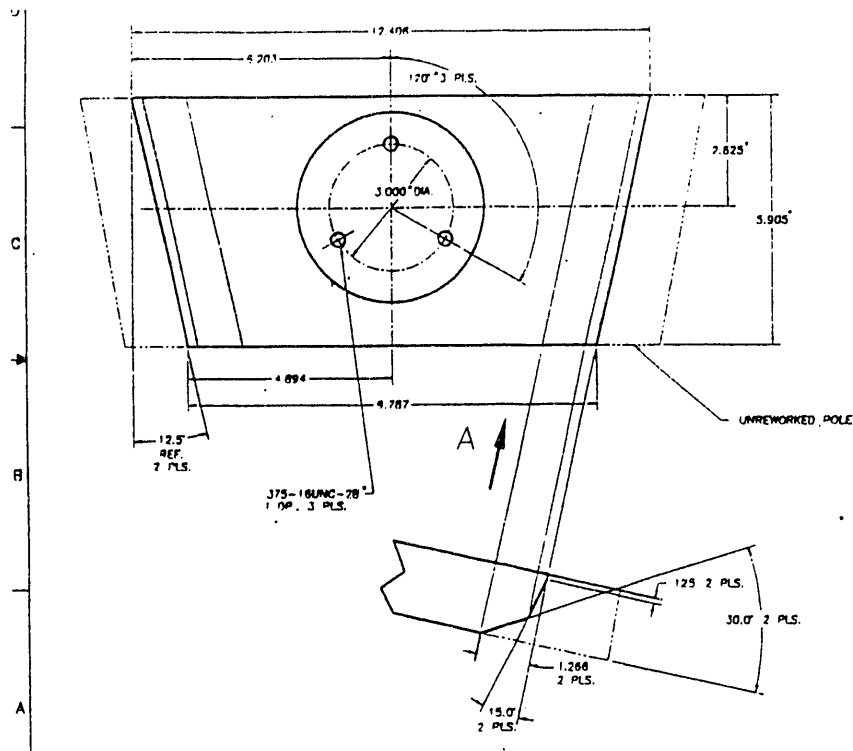
Fig. 2 Dipole pole piece.

The dipole was measured at the NSLS Magnetic Measurement lab. Hall probe measurements of the magnetic field along a line normal to the entrance face[5] are shown in Fig. 3. The probe entered the magnet at the center of the poleface width. These measurements confirmed that the magnetic edge of the magnet corresponded with the physical edge of the pole piece to within 1% of the total effective length.

Table 2 Dipole properties		
bend angle	25	degrees
radius of curvature	64.60	cm
effective length	28.19	cm
sagitta	1.53	cm
B for 50 MeV/c	2.581	kGs

The excitation curve for the magnet is shown in Fig. 4. The Hall probe was located at the maximum field location[6] of Fig. 3. The field is linear with current up to about 2 kGs, after which saturation of the steel pole piece is clearly evident.
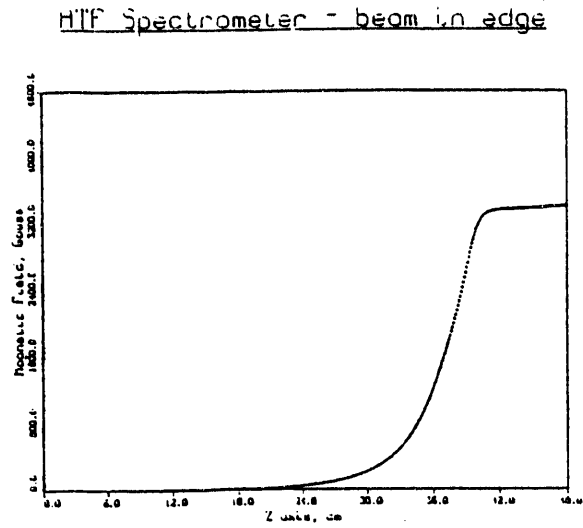
HTF Spectrometer - beam in edge

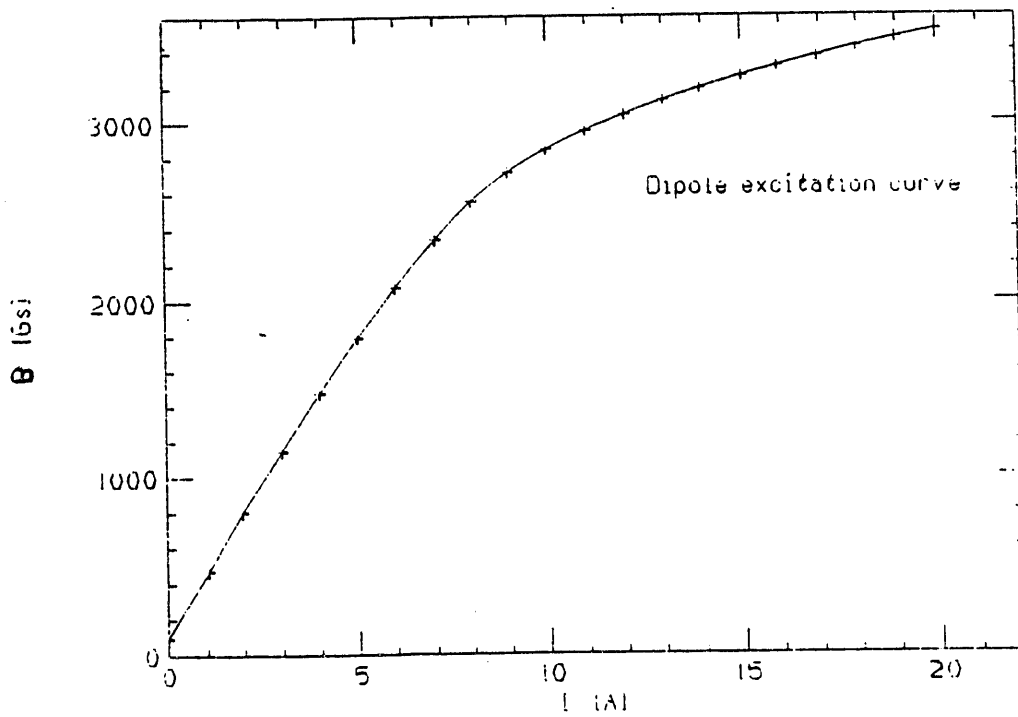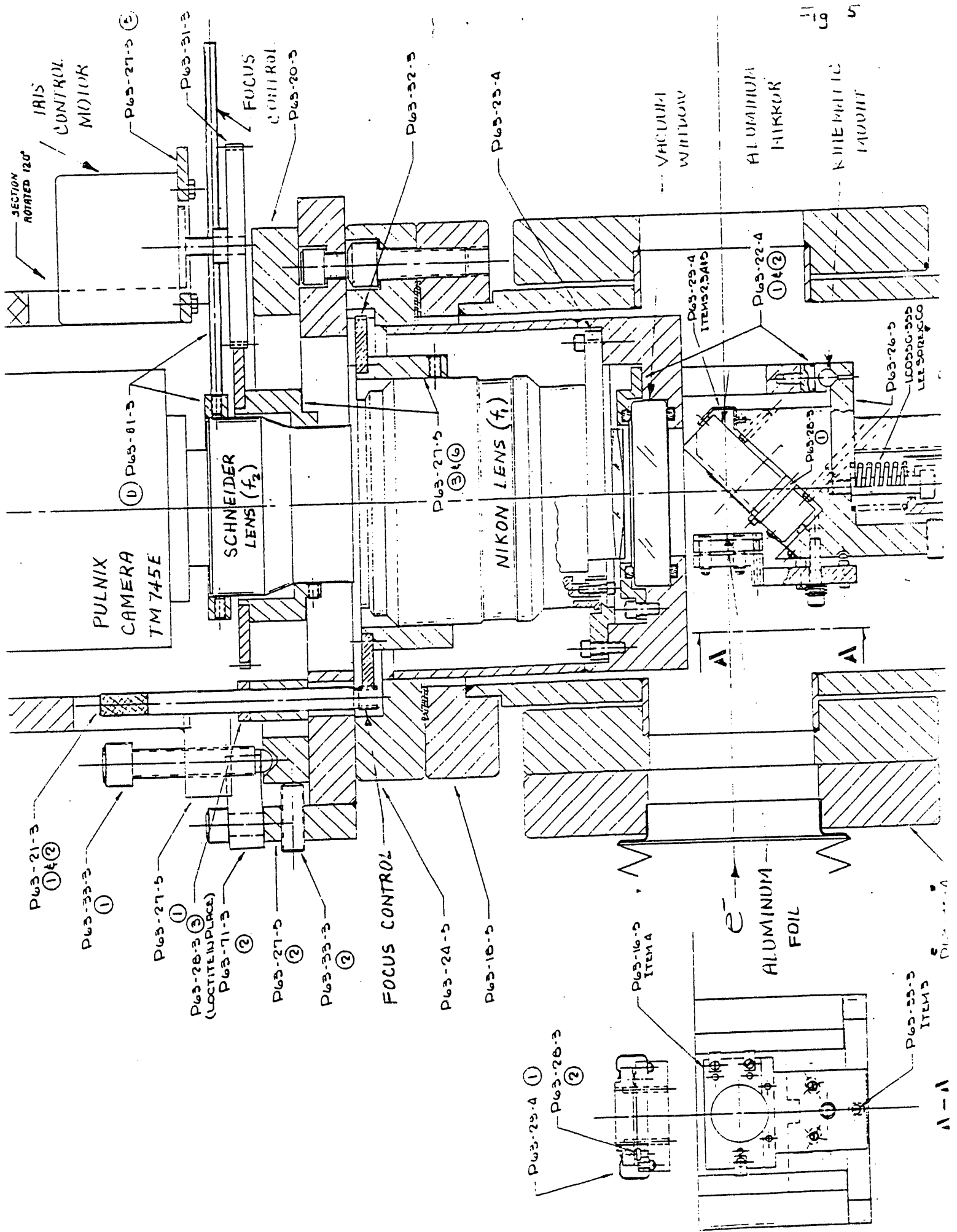Fig. 3 Magnetic field in the dipole along trajectory perpendicular to the entrance face.

Fig. 4 Magnetic field in the dipole as a function of excitation current.

3 Profile monitor assembly

The profile monitor is used to visually detect the electron beam at the exit of the spectrometer[7,8]. Fig. 5 shows a drawing of the profile monitor assembly. The beam first encounters an Al foil mounted perpendicularly to the beam axis. The exit side of the foil has a ≈15 mm diameter, layer of Gd_2O_2S:Tb phosphor. Scintillation light from the phosphor reflects from the 45° mirror and passes through a vacuum window to the optical collection system. In the normal case this consists of a pair of lenses, f1 (Nikon) and f2 (Schneider), that make a point-to-point focus of a point on the phosphor to a point on the CCD camera (Pulnix model TM-745E). About 3% of the light is collected by the first lens and the transmission efficiency to the CCD is ≈75 %. Approximately 4 charges are produced in a CCD pixel for each incident beam electron[7,8].

The electron beam passes through the Al mirror on its way to the Faraday cup at the end of the beamline. A diagram of the Faraday cup is shown in Fig. 6. The mirror cannot be extracted like those in other ATF profile monitors, so the downstream side of the mirror was hollowed out. Table 3 shows a number of properties of the profile monitor system.

Table 3 Profile monitor properties		
phosphor thickness	30	μm
phosphor density	3	g / cm^3
phosphor grain size	10	μm
phos 10% decay time	1.2	ms
Al foil thickness	25	μm
Al mirror thickness	0.062	in
focal length f_1	36	mm
focal length f_2	25.7	mm
magnification	0.71	
CCD active area	8.4 x 6.4	mm
spatial resolution	50	μm
min observ beam inten	2×10^6	mm^{-2}

IRIS / CONTROL MOTOR

SECTION ROTATED 120°

P63-27-5 (E)

P63-31-3

FOCUS CONTROL

P63-20-5

P63-32-5

P63-23-4

P63-01-5 (D)

SCHNEIDER LENS (f_2)

PULNIX CAMERA TM 745E

P63-27-5 (3)(6)

NIKON LENS (f_1)

P63-29-4 ITEM 2,5 AID

VACUUM WINDOW

ALUMINUM MIRROR

KINEMATIC MOUNT

P63-22-4 (1)(2)

P63-26-3 (1)

P63-26-5 LOOSE 355 LEE SPRING CO

P63-21-3 (1)&(2)

P63-33-3 (1)

P63-26-3 (3) (LOCTITE IN PLACE)

P63-71-5 (2)

P63-27-5 (1)

P63-27-5 (2)

P63-33-3 (2)

FOCUS CONTROL

P63-24-5

P63-16-5

A

A

ALUMINUM FOIL

P63-16-5 ITEM 4

P63-23-4 (1)

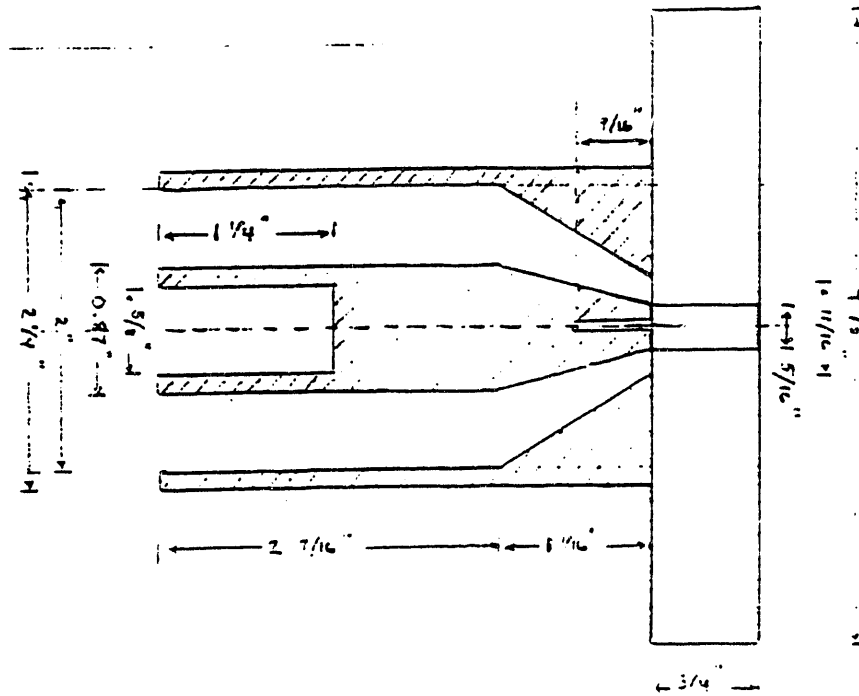P63-26-3 (2)

P63-33-3 ITEM 3

A — A

Fig. 5

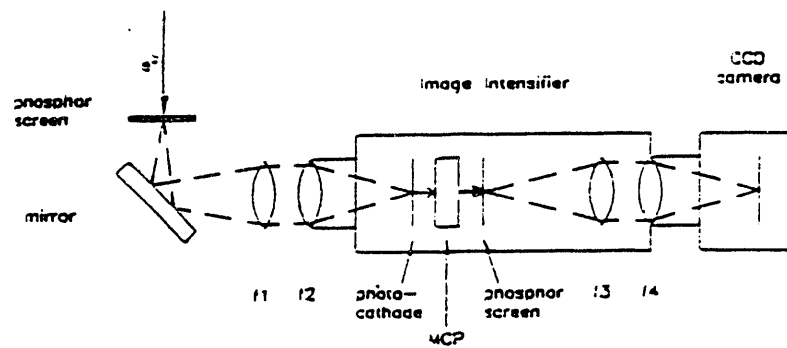Fig. 6   Schematic diagram of the Princeton Faraday cup.

Fig. 7   Profile   monitor   optics   with   the   image
intensifier[7].

In situations where the beam spot is expected to be diffuse or
where the total charge in the beam is small, an optional image
intensifier can be used before the camera in the profile monitor.
The intensifier, shown schematically in Fig. 7 and provided to the
ATF by Princeton University, is a Paterson Electronics model LPQ50.
It uses a 25 mm, electrostatically focused microchannel plate. The
gain is adjustable from 10000 to 50000. It is possible when using
the intensifier to see single electrons with the profile monitor.
The intensifier adds an additional contribution to the spatial
resolution of 20 μm. This gives an overall spatial resolution of 55
μm when added in quadrature to the fundamental resolution of 50 μm
given in Table 3. Lens f3 has a focal length of 50 mm, while f4 has
35 mm. Since this lens combination also has a magnification of 0.7,
the overall magnification from the phosphor screen to the CCD
camera is 0.50.

4 Expected performance

We describe here typical values for the acceptances and resolution
expected with this spectrometer. Some of these quantities are
dependent on the actual geometrical layout of the experiment and
the actual quadrupole settings.

Angular acceptance

We consider the non-bend plane acceptance for the case of the ICA
experiment. The beampipe inner radius is 1.26 cm. The first
focussing quad in this plane is GQ15, whose entrance is located at
a distance of 3.17 m from the center of the ICA gas cell. Thus the
spectrometer should accept electrons leaving the ICA interaction
region with deflections of up to ± 4.0 mR in the non-bend plane[9].

Momentum acceptance

Consider an electron beam with mean momentum p. The change in
bending angle α through dipole GD2 due to a change in momentum is
given by

$$\Delta\alpha = \alpha \frac{\Delta p}{p} \qquad (1)$$

This gives rise to a transverse displacement downstream of the
dipole of

$$\Delta x = D \Delta\alpha \qquad (2)$$

where D is the distance from the center of the dipole to the center

of the first bending plane focussing quad GQ14. The momentum range accepted by the spectrometer is

$$\Delta p = \frac{\Delta x}{\alpha D} p \qquad (3)$$

Using Δx = 1.26 cm for the beampipe inner radius, D = 83.2 cm, and a central momentum p = 45 MeV/c, we find that the momentum range accepted by the spectrometer is ± 1.6 MeV/c.

For an optimal design the momentum measurement range on the profile monitor screen should match the momentum acceptance above. The transverse displacement caused by momentum spread is given by the R_{16} matrix element in TRANSPORT. The nominal spectrometer tune has

$$R_{16} = 2.0 \frac{mm}{\%}$$
$$= 4.4 \frac{mm}{MeV/c} \qquad (4)$$

where the second line applies to a central momentum of 45 MeV/c. Using a screen half-width of 7.5 mm, this gives a measured momentum range ± 1.7 MeV/c.

Momentum resolution

We define the momentum resolution to be the smallest measurable momentum change. Taking 50 μm to be the spatial resolution of the profile monitor, and using the nominal R_{16} = 4.4 given above, the momentum resolution of the spectrometer is 12 keV/c.

Beam profile

We give an example beam profile through the spectrometer in Fig. 8. The figure shows the 1 sigma beam envelope in the bend and non-bend planes versus axial distance Z for the ICA experiment. Z = 0 corresponds to the exit window of the ICA gas cell. The curves extend to Z $\approx$ 360 cm, which corresponds to the screen in the profile monitor detector. The quadrupoles produce point-to-point focussing in the bend plane (the starting beam size is not actually a point because of multiple scattering in the gas and windows).
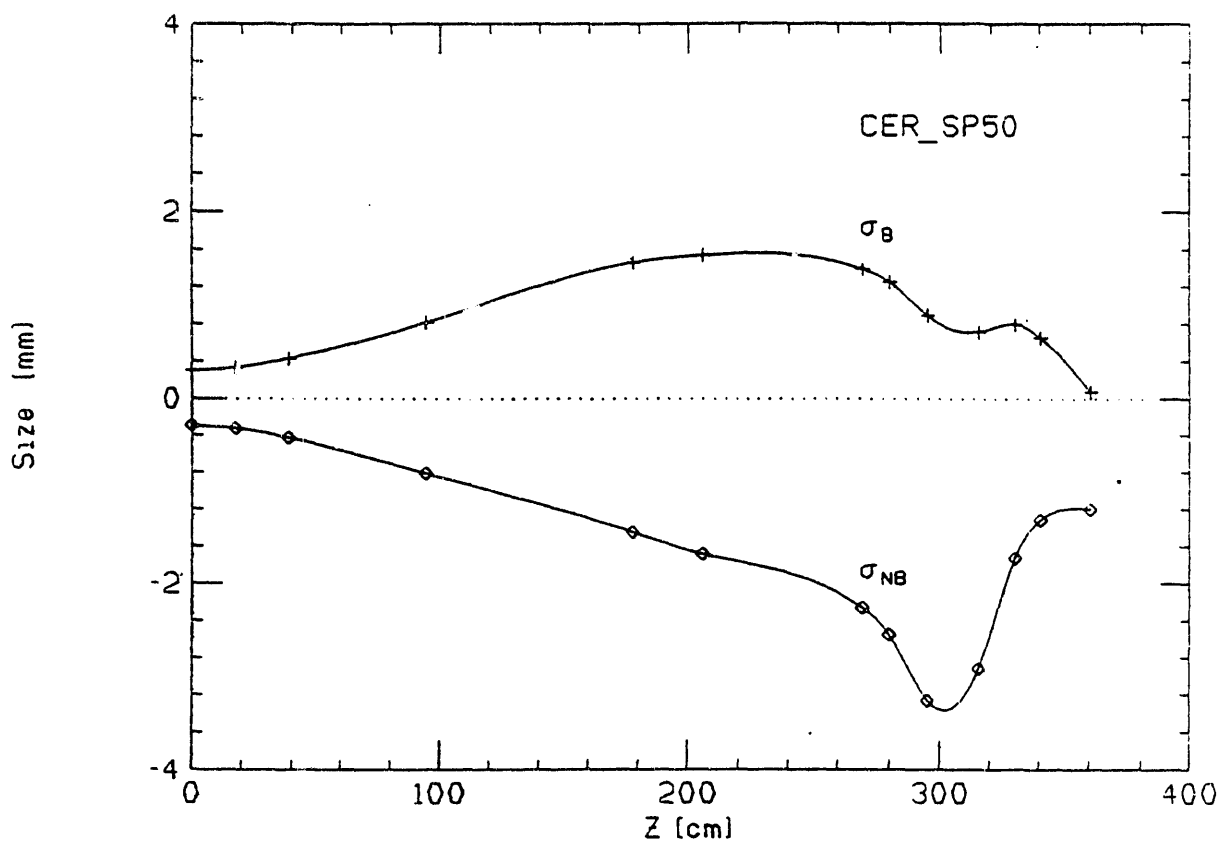
Fig. 8   Beam profiles in the bend (B) and non-bend (NB)
planes   in   the   analysis   spectrometer   for   the   ICA
experiment.

Acknowledgements

Notes and References

[1] W. Kimura et al, *Inverse Cerenkov laser acceleration experiment*, Spectra Technology Inc. note DE-AC06-83ER40128, 1989.

[2] W. Chen et al, *Proposal for a study of laser acceleration of electrons using micrograting structures at the ATF*, Brookhaven National Laboratory report, BNL-43465, 1989.

[3] K.T. McDonald et al, *Proposal for an experimental study of nonlinear Compton scattering*, Princeton University note DOE/ER/3072-55, 1989.

[4] The quadrupoles were located in front of the dipole in the original Grating Acceleration experiment designs. See for example, R.C. Fernow, *Updated 50 MeV spectrometer design*, informal report RCF-LA-8602, 1986; R.C. Fernow, *Scintillating fiber detector for the grating acceleration spectrometer*, informal report RCF-LA-8801, 1988. This arrangement would have allowed a range of momentum acceptances to be covered by adjusting the distance between the dipole and the profile monitor. The design was changed in 1989 with the quads moved downstream of the dipole to accommodate simultaneous running of the Grating Acceleration and Compton scattering experiments.

[5] Note that this measurement path crosses the exit edge at an angle of 25°.

[6] The location of the true maximum field was measured to be 13 mm transverse to this point, where the field was 1.2 Gs higher.

[7] D.P. Russell III, *High-brightness electron beam production at the Brookhaven Accelerator Test Facility*, Dissertation, Princeton University, 1992; DOE/ER/3072-67. Chapter 7 describes the profile monitor system, including the image intensifier.

[8] D.P. Russell & K.T. McDonald, *A beam profile monitor for the BNL Accelerator Test Facility*, 1989 Part. Acc. Conf.; DOE/ER/3072-52.

[9] This ignores the defocussing effect of the preceding quad GQ14. The extra divergence is negligible for the standard ICA beam tune.

Appendix: magnet excitation curves

For completeness we include here excitation curves for each type of magnet used in the spectrometer. The short and long SLAC quads following the dipole are integral parts of the spectrometer assembly. The long Chinese quads, located upstream of the dipole, can optionally be used for some experimental arrangements. The quadrupole excitation curves are taken from X. Wang & C. Sylvester, *Quadrupole magnets measurements*, informal report, BNL-45801.

Table A1 Excitation curve for GD2 dipole		
I [A]	B [Gs]	p [MeV/c]
0.000	95.6	1.85
1.034	471.3	9.13
1.964	802.5	15.55
2.986	1149.0	22.26
3.985	1477.7	28.63
4.995	1789.6	34.68
5.988	2077.0	40.24
7.002	2343.0	45.40
7.973	2553.3	49.47
8.971	2716.9	52.64
9.980	2845.0	55.13
10.977	2949.6	57.15
11.998	3041.9	58.94
13.026	3123.7	60.53
13.962	3190.8	61.83
15.016	3259.4	63.15
15.931	3314.0	64.21
16.950	3370.4	65.31
17.992	3423.7	66.34
18.996	3471.0	67.25
20.000	3514.7	68.10

Table 9 The excitation table for Chinese quadrupole type 2 no. 3.

Current(A)	Gradient(Gauss/cm)
3.5	79.22295
7.0	159.327575
10.5	238.0729
14.0	317.5825
17.5	395.99225
21.0	475.09525
24.5	552.581

Table 10 The excitation table for short SLAC quadrupole 153.

Current(A)	Gradient(Gauss/cm)
0.7	136.3408
1.4	252.5708
2.1	377.4048
2.8	493.424
3.5	612.8535
4.2	731.4085
4.9	849.028
5.6	964.5245
6.3	1080.4165
7.0	1186.6385

Table 11 The excitation table for long SLAC quadrupole 135

Current(A)	Gradient(Gauss/cm)
0.7	141.34233
1.4	257.78066
2.1	377.929333
2.8	499.5900
3.5	621.3633
4.2	743.160667
4.9	866.03733
5.6	988.611667
6.3	1109.4165
7.0	1226.52866

END

DATE
FILMED
5/27/93